Surface Layer Turbulence and Aerosol Profiles During MAPTIP

K. L. Davidson
P. A. Frederickson
Department of Meteorology
Naval Postgraduate School
589 Dyer Rd., Room 254
Monterey, CA 93943-5114
USA
Tel: 408.656.2309 Fax: 408.656.3061 EMail: davidson@osprey.nps.navy.mil

Gerrit de Leeuw
TNO Physics and Electronics Laboratory
Oude Waalsdorperweg 63
2597 AK The Hague
The Netherlands

SUMMARY

The Naval Postgraduate School (NPS) and the TNO Physics and Electronics Laboratory (TNO-FEL) deployed in situ sensors near and on Meetpost Noordwijk (MPN) during MAPTIP to describe the surface layer processes and also to evaluate models for near-surface aerosol profiles. Vertical profiles of aerosol counts were measured on the MPN tower by TNO-FEL with Rotorod impaction samplers. The aerosol distribution measurements were made for 10 radius bins, with centered radii ranging from 6.5 to 75 μm. Atmospheric surface-layer turbulence and stratification were measured by NPS from an instrumented buoy that was located a short distance from MPN. Existing models relate aerosol profiles to source, sink, and turbulent transport processes. The assumed source process is bursting air bubbles at the surface. The removal processes are turbulent deposition and gravitational fallout. Turbulent transport is described by the friction velocity and the near-surface stratification. The combined buoy and MPN data sets are shown to provide valuable descriptions of surface layer properties during the variable period from 26 October through 3 November. Results from eleven profile sampling periods were compared with model predictions for which buoy measured parameters and aerosol sizes were inputs. The predicted concentration often decreased more with height than observed. This is believed due to the coastal input to the aerosol source since advected aerosol would reduce influences on gradient of bubble production at the surface.

1. INTRODUCTION

Describing height variations of aerosol size spectra in the surface layer is important to both understanding thermal imaging results from MAPTIP and to understanding processes important in modeling of aerosol, in general. Surface layer aerosol properties described by existing equilibrium models, i.e. NOVAM [1], are based on empirical data and can be assumed to apply to a level some distance above the surface, around 10 meters. For imaging of targets near the horizon, some knowledge of vertical gradients are necessary to take into account a path that traverses layers extending from the surface and up. Models for aerosol in the marine boundary layer are based on source/sink, transport (mixing), and chemistry characteristics. Processes affecting aerosol are expected to increase/decrease from the boundary, i.e. in the vertical. Relative humidity will decrease from the ocean surface which is also the source of bubble produced sea-salt aerosol. It is also the sink if removal is by gravitational fall-out and turbulent deposition. Turbulent mixing would diminish the strengths of the gradients produced by the surface's dominant role in the processes. However, accurate measurement of aerosol profiles (gradients) are as appropriate for evaluation of model performances as are aerosol concentrations themselves. For this to be true, the turbulent processes (mixing and deposition) have to be accounted for.

We will describe the results from examinations of near-surface aerosol profiles measured during MAPTIP relative to transport and removal processes, available through measurement or calculated from the data. We will also present atmospheric surface layer properties, as measured from MPN and the NPS buoy, during MAPTIP. The latter show the wide range of wind forcing and stability conditions affecting MAPTIP and important to all interpretations of the collaborative obtained data bases.

An expression for given aerosol radius concentrations, X_i, at two different heights, Z_i, where i = 1 and 2, is [2,3]

$$Ln(X_2/X_1) = -[V_d/ku_*]\,[Ln(Z_2/Z_1) - \Psi(Z_2/L) + \Psi(Z_1/L)] \quad (1)$$

u_* is the surface-layer friction velocity, $\Psi(Z_i/L)$ is an empirically formulated scaling expression, e.g. Businger et al. [4], L is the Monin-Obukhov stability length, and V_d is a removal velocity that depends on turbulent deposition and gravitational settling [5]. By convention, V_d is positive if the aerosol is falling. This expression was formulated by Toba [6] with the assumption of a balance between surface production and removal, no horizontal advection, and constant turbulent vertical transport. Eqn (1) extends Toba's formulation to include non-neutral stratification but neglects the relative humidity influence on aerosol size. The latter could be important if the very near-surface, $Z <$ 2 meters, gradients are being considered or if relative humidity is close to 100%.

The Eqn (1) predicted gradient depends on aerosol size because of V_d which is the sum of gravitational settling and turbulent deposition velocities, [5]. Gravitational settling depends on aerosol density and the radius squared, r^2, and turbulent deposition depends on u_* as well as the radius.

Paper presented at the Sensor and Propagation Panel Symposium on "Propagation Assessment in Coastal Environments" held in Bremerhaven, Germany 19-22 September 1994.

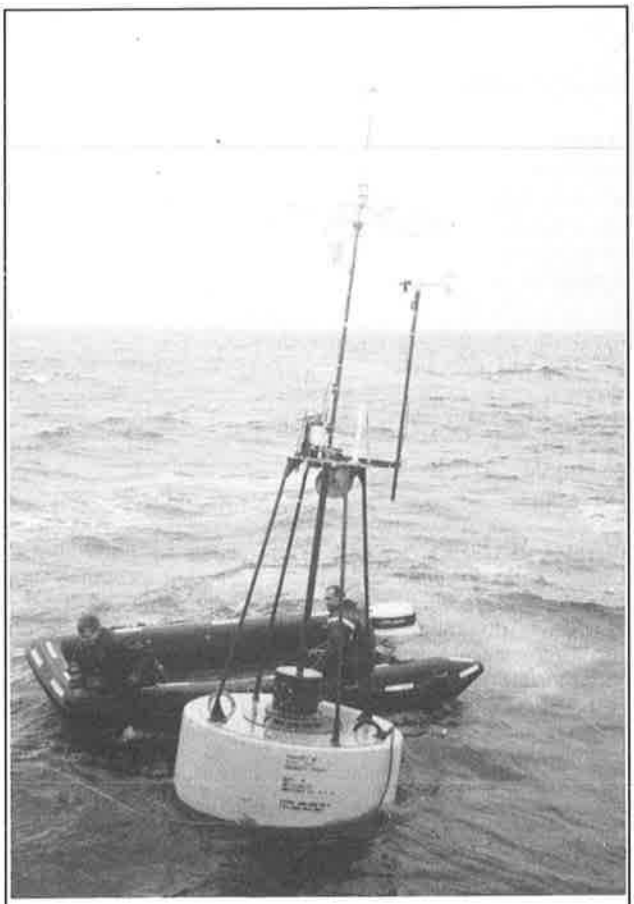

Figure 1.
NPS surface-flux buoy being deployed NW of MPN, top of mast is 5 m above water line

2. NPS BUOY AND SURFACE LAYER CONDITIONS DURING MAPTIP

2.1. Buoy Deployment and Turbulence Calculations

The NPS buoy, Figure 1, was deployed at fixed location approximately 560 meters northwest of MPN, Figure 2. Its first deployment was at 1500 UT on 11 October. At that time, continuous mean and turbulent wind and virtual temperature measurements were made with a sonic anemometer (Solent) mounted atop a mast 5 meters above the water surface. Mean wind speed and direction measurements were also made with a propeller and vane (R. M. Young) located on the mast 4 meters above the water surface. Sea temperature was measured with a thermistor located approximately 0.5 meters below the water surface but yielded unexplained variations from the MPN measured values. Also, relative humidity and atmospheric pressure measurements could not be recorded, even at the time of initial deployment, due to a computer board failure.

At about 1130 UT on 12 October, less than 24 hours after initial deployment, a severe storm occurred and combined wave and wind effects cased the buoy sensors and inboard computer system to be damaged. Even though it was a short period, and not within the MAPTIP intensive observation period (MAPTIP-IOP), examination of data collected during the period was important to understanding the buoy's usefulness.

The buoy was redeployed near 1300 UT, 26 October with the sonic but no other systems working. Data not available from the operating buoy systems but necessary for estimating Z/L, i.e. humidity and sea temperature, were available from MPN. The buoy operated successfully until recovered at 1000 UT on 4 November, and provided data for 12 of 18 of the aerosol profile sampling periods.

The two boundary layer parameters necessary to describe the aerosol profile, according to Eqn (1), are the friction velocity u_* and L. Variance spectra, $S_u(f)$, were calculated from sonic anemometer turbulent wind records and used to calculate u_* values on the basis of the inertial-dissipation method. The method's value for shipboard or buoy application is that it is based on the high frequency portion of the spectrum which is not affected by wave-induced platform motion. The method was that used previously with the buoy system, Skupniewicz and Davidson [7]. The Monin-Obukhov stability length, L, necessary for the inertial dissipation method as well as in Eqn. (1), was calculated with mean wind, temperature and humidity values.

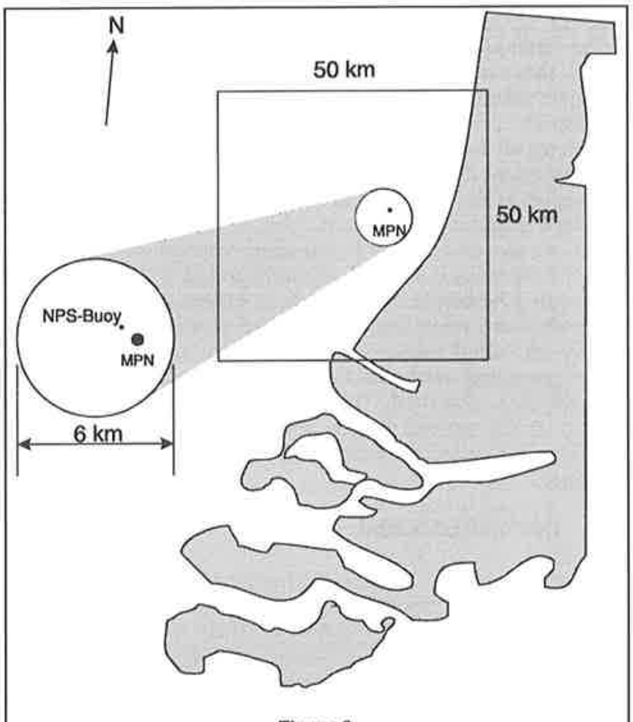

Figure 2.
Relative locations of MPN to The Netherlands coast and NPS buoy to MPN.

These were those from MPN mounted sensors since, as mentioned previously, buoy relative humidities and eventually both air and sea temperatures were not available during the MAPTIP-IOP.

Applications of surface layer similarity flux-profile relationships yield [8] the following inertial-dissipation based relation between u_*, Z, Z/L, $S_u(f)$, f and U.

$$u_* = [S_u(f) f^{5/3} / (\alpha U^{2/3})] \; [kZ/\Phi_\varepsilon(Z/L)]^{1/3} \qquad (2)$$

U was the sonic measured mean wind speed. Φ_ε is a dimensionless stability function, and α is an empirical constant. Our selections for the function and constant were those described by Edson et al [9] and formulated on the basis of MPN tower data. Also Z/L, based on mean MPN data with a bulk method, was calculated using the drag coefficient and turbulent heat (sensible and latent) exchange coefficients described by Smith et al [10] which also were formulated from an earlier experiment at MPN.

Wind speeds from MPN and the buoy, scaled to 10 meter height, and bulk and inertial-dissipation u_*'s for the period 11-12 October period are shown in Figure 3. The quality of the sonic measured wind speed from the wave-influenced buoy platform is an important consideration in the evaluation of its performance. The range of wind speed encountered during the initial deployment period allowed an excellent evaluation of the buoy systems, including mooring procedures, for estimating u_* via the inertial dissipation method.

The MPN (solid lines) wind speeds and NPS buoy wind speeds measured by a propeller anemometer (dashed) and the sonic anemometer (dotted) are in good agreement until storm winds occurred after 0600 UT on 12 October.

The NPS (buoy) sonic anemometer failed at approximately 1020 UT on 12 October, when the winds reached a speed of 15 m/s. Also, at that time the NPS propeller winds become lower than the MPN winds, by as much as 5 m/s, until the storm subsided at about 1800 UT 12 October. This may have been caused by the buoy leaning at a large angle because of high storm winds which resulted in the propeller not measuring the full horizontal wind speed. A conclusion reached from this was the that sonic anemometer would provide accurate mean and turbulent wind values over the wide speed ranges expected.

Traces in Figure 3b indicate that during this initial deployment period the buoy (sonic anemometer) measured air temperature had a bias, near 1 °C lower than the MPN air temperature, after both were scaled to the 10-meter height. However, the buoy air temperature tracked the MPN temperature extremely well. Since the buoy bias was viewed to be correctable to MPN with further analyses of the sonic transmitter/receiver spacing, we believe the MPN values can be applied to the buoy location. Examination of Figure 3b reveals that the MPN-buoy sea temperature difference was variable, with the buoy sea temperature contributing most to the variability and being between 1-1.5 °C lower.

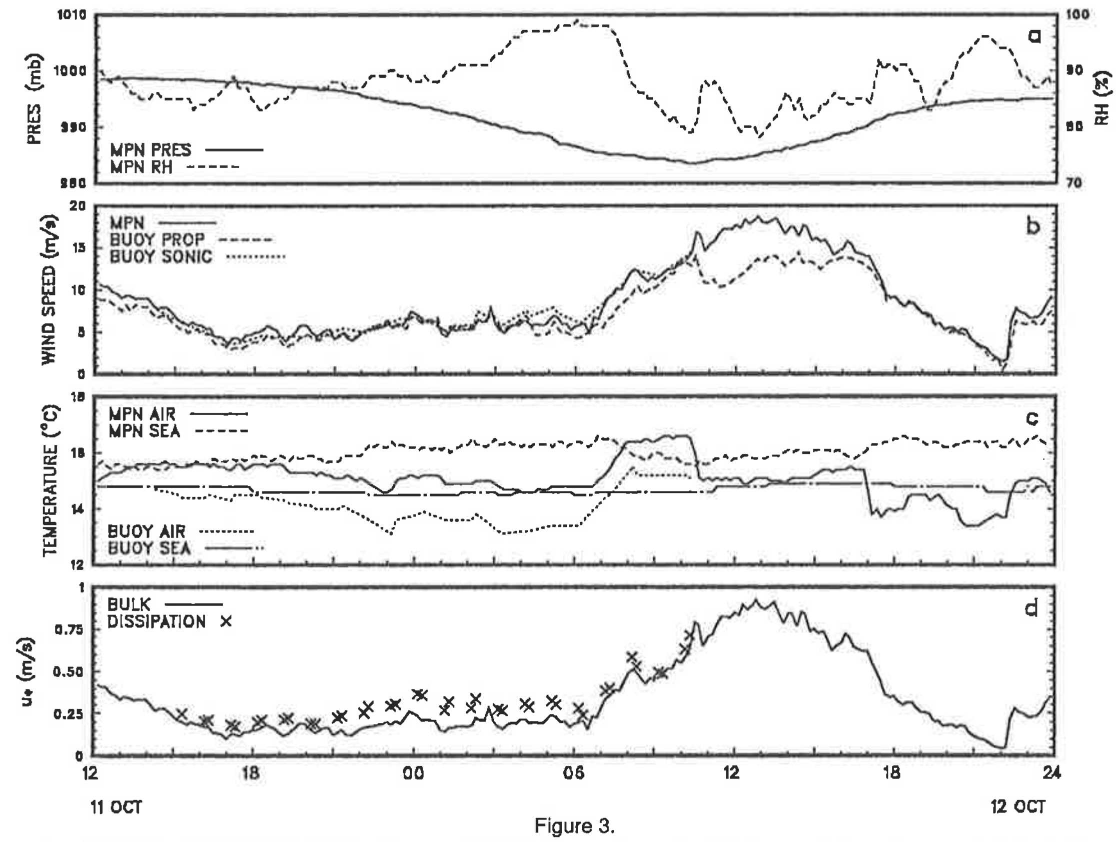

Figure 3.
Time series (10/11/00 - 10/13/00 UT, 1993) of buoy and MPN measured and calculated parameters, a) pressure and relative humidity, b) 10-meter wind speed, c) air and sea temperature, d) bulk [10] and dissipation u_*

So again, it was decided to use the MPN values to represent the buoy location. A conclusion reached on the basis of comparisons between these buoy and MPN data was that MPN mean wind, humidity, and air and sea temperature values were sufficient in determining stability, Z/L, for the buoy location.

The x's in Figure 3c are u_*'s calculated with the inertial-dissipation method and, of course, end with the failure of the sonic anemometer at 1020 on 12 October. The solid line in Figure 3c was drawn to u_*'s calculated with mean MPN data using the bulk formulations based on previous MPN data [10]. For 9 hours (11/21 to 12/06 UT), buoy inertial-dissipation u_* values are 10-20% higher than the bulk friction values based on MPN data. However, the NPS friction velocity values are in excellent agreement with the bulk values during the storm which arrived shortly after 0600 UT 12 October, until the NPS sonic anemometer failed at 1020 UT 12 October. Further, the error during the preceding 9-hour period is not considered serious since the bulk formulation used does not take into account wave-age influences which should cause u_* to be larger during a increasing wind speed.

2.2 MAPTIP-IOP Surface-Layer conditions

The collaborative MAPTIP measurement period began on 19 October. Significant personnel and ship efforts were made to have the buoy recovered, to have repairs/replacements made, and to have it redeployed. This was because the turbulence data were considered key parameters for descriptions of the surface layer processes. Post-storm evaluations of the buoy revealed that the system could be repaired to collect mean and turbulent wind and temperature from the sonic anemometer, without having to wait for parts to arrive. Hence, to avoid further delay, the buoy was redeployed near 0000 UT, 26 October with the sonic but no other sensor systems working. Data not available from the buoy but necessary for Z/L calculations were available from MPN. They were shown to be representative for the buoy location in above discussions.

The buoy operated successfully until recovered near 1000 UT on 4 November. It provided data for 7 of 12 of the aerosol profile sampling periods with acceptable wind directions, listed in Table 1.

There were a total of 18 aerosol profile sampling periods but 6 of these occurred with wind directions that were determined to be too influenced by MPN's structure. The Table 1 profile period list is sorted according to wind direction. Occurrences of positive slopes, X_i in Eqn (1) increasing with height, are marked for purposes of later discussions.

Time series measured at both buoy and MPN for the 26 October - 4 November period appear in Figure 4. Symbols along the bottom of Figure 4 d mark times with aerosol profiles, listed in Table 1. Mean parameters from both platforms are shown in the time series because Z/L was estimated from MPN winds, temperatures and humidity and because u_* was estimated from buoy (sonic) mean and turbulent winds.

MPN and buoy wind speeds and air temperatures in Figure 4 were all scaled to a 10-meter reference height. The scaled buoy wind speeds are generally within (always higher than) 1 m/s of MPN wind speeds. The two platforms are in good agreement during the period of winds less than 5 m/s, from about 10/30/1800 UT to about 11/03/1200 UT. The buoy air temperatures are generally within 1 ^oC (always lower) than MPN's until about 10/28/1800 UT, after which they agree very well. We believe differences between the two locations, in both air temperature and wind speed, become more important at lower wind speeds because then the differences have more influence on Z/L, an important parameter in the tested model. Fortunately, the platforms were in good agreement during the time of lower wind speeds.

As was the case for the first deployment, the buoy obtained inertial-dissipation u_* values are often higher than the bulk u_* values, calculated with MPN-based exchange coefficients. This is not always the case however, the buoy values have the appearance of being always higher because they are indicated with x's and the bulk values being are with a thin line. There are no times when the two differ by factors of two which occurs when storms fronts move through. One of the reasons the bulk values are in such apparent agreement is that the applied C_{D10N} formulation was from MPN, [10]. Such agreement in these results will lead us to confidently use MPN bulk u_* values when aerosol profiles are available but not buoy u_*'s.

Table 1. MAPTIP Profile Periods

date/time mo/day/UT	Wdir (^oD)	U m/s	RH %	Tair C	Tsea C	Radius (μm) 8	12	16	21	28	38	50	63	Tot	8-21 μm	28-62 μm
10/25/0705	28	9.3	74	10.6	11.5	x	x							2	2	0
10/26/1712	31	5.9	81	9.8	11.5		x	x	x					3	2	1
10/26/0848	37	7.8	81	12.1	11.3	x	x					x		2	2	0
10/19/1346	48	2.1	55	7.4	13.5	x	x	x	x	x	x	x		7	4	3
10/27/1030	52	5.5	86	9.5	11.6									0	0	0
10/24/0834	53	11.9	65	6.9	11.7	x	x	x	x		x			5	4	1
10/24/1310	54	10.7	65	8.8	11.7	x	x					x		3	2	1
10/22/1039	61	8.6	76	8.4	12.4	x	x	x	x	x				5	4	1
10/30/1600	65	6.6	95	5.2	11.3			x	x	x				3	2	1
10/28/1611	72	5.5	82	8.7	11.7		x	x	x	x	x			5	3	2
10/29/1328	74	6.5	87	7.7	11.5			x	x	x	x	x		5	2	3
10/28/1121	85	6.2	78	9.4	11.7	x		x	x	x		x		5	3	2
					Total Positive	7	8	8	8	6	4	5	0	46	31	15
					Total Profiles	12	12	12	12	12	12	9	2	83		
										Percent Positive				55%		

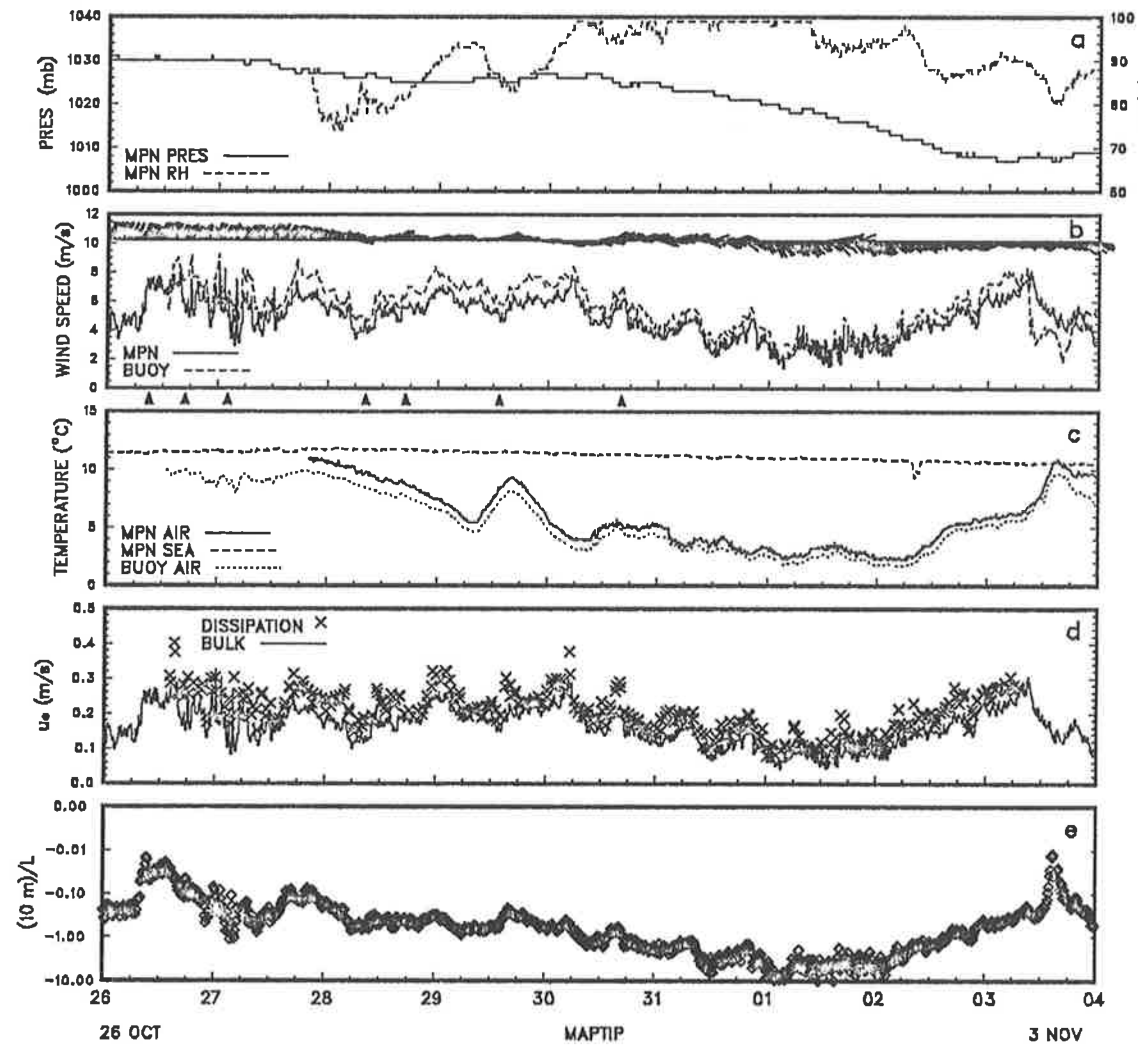

Figure 4.
Time series (10/26/00 - 10/04/00 UT, 1993) of buoy and MPN measured and calculated parameters, a) pressure and relative humidity, b) vector wind where barbs are from MPN, c) air and sea temperature, d) bulk [10] and dissipation u_*, e) Z/L where Z = 10 m. Symbols between panels b) and c) mark valid aerosol profile sampling periods.

Time series in Figure 4 show the wide range of wind and thermal stratification that occurred over the time when the buoy data were available. This range was cause by a synoptic-scale cyclone (low pressure center) approaching MPN most of the period with passage on 3 November, Figure 4 a..

Relative humidity, Figure 4a, was near 100% for two days, 30-31 October, and could affect our neglect on relative humidity's role on aerosol gradient. As the low approached, winds generally decreased through 1 November when they increased as the low center passed south of the MPN North Sea location. Also with the low's passage, winds turned clockwise from NE through SE. The evolving wind direction caused the airflow to be partially from the North Sea for 26 October, from off-shore but still not through MPN for 27-30 October, and through MPN for 31 October - 3 November.

The wind direction being through MPN led to no post-30 October aerosol profiles being examined, Table 1. Therefore, aerosol profiles were examined for a period (10/26/1200 -10/30/1600) when winds speeds were high enough to expect active surface production. Aerosol profiles were also examined for the times in the preceding week (19-25 October) when winds were E-NE and except for 10/19 high enough for surface production, Table 1. Air and sea temperatures and 10/L time series in Figures 4c and 4b reveal the thermal stratification to certainly have been unstable. With 10/L approaching -1, convective mixing will have an influence on aerosol profiles.

We also use the neutral drag coefficient, C_{DN}, in our evaluation of the u_* measurements. C_{DN} is u_* normalized for both wind speed U and stratification, z/L. according to the following expression,

$$C_{DN}(z)=[(u_*/U)+\psi(z/L)/k]^{-2}, \qquad (3)$$

where $\psi(z/L)$ is a flux-profile related function.

Since C_{DN} depends on height, the calculated neutral drag coefficients were extrapolated to a reference level of 10 meters and are denoted as C_{D10N}.

Figure 5 has a comparison of buoy inertial-dissipation and MPN bulk derived C_{D10N}'s , Figure 5b, relative MPN water-level departures from mean tide, and Figure 5a. The water (tide) height and C_{D10N} variation are correlated because wind speed was not adjusted for the tide-influenced surface current. These results provide evidence on the accuracy of the u_* estimates since C_{D10N}'s calculated from them reflect the non-removed surface current

3. TNO-FEL AEROSOL PROFILES

Size distributions of particles larger than 5 µm in radius were measured with a Rotorod inertial impactor. The sampler consists of two polished stainless steel rods, mounted in a retracting collector head on a motor which rotates at a nominal speed of 2400 rpm. The linear velocity of the rods is 10 m/s. Particles impacted on the rods are retained by a sticky coating (silicone).

Microscope images of the rods are digitized to determine the particle size distribution by computer, [11]. Impaction and magnification limits determine the 5 µm radii and larger sizes range. Concentrations were estimated for up to 10 radii bins; centered at 6.5, 8.5, 12, 16, 21, 28, 37.5, 50, 62.5, and 75 µm.

Profiles were defined on the basis of up to 7 fixed-heights (1, 2, 3, 5, 7, 9, 11 meters) above mean tide height and of up to 7 levels (from .5 to 2.0 meters) above a wave follower. We consider profiles from the "fixed" levels only because Eqn. (1) is not based on wave-following scaling. Profiles were possible for up to 9 different radii but numbers were often too small to be statistically significant to define them for largest sizes.

A typical set of MAPTIP profiles, corresponding to 13:28 UT on 29 October, is shown in Figure 6a, with linear regression lines to the Ln versus Ln distribution. The Ln(DN/dD, i.e. X_i) versus Ln(Z_i) display and regression are based on the Eqn. (1) prediction. DN/dD is the number of aerosol per diameter interval per volume. A typical set of profiles, corresponding to 1510 UT on 24 September, from the MPN based (September 1993) Air-Sea Gas Exchange (ASGASEX) experiment [12] is shown in Figure 6b. ASGASEX results enter into the final discussions of MAPTIP results. Table 2 lists ASGASEX profile sampling periods for periods when the wind direction was determined to be acceptable, counter-clockwise from 090 - 180 deg. Table 2 is similar to Table 1 for MAPTIP in that it includes measured mean parameters and indicators of positive slope occurrence according to radii. It differs in that the Table 2 profile list is sorted according to wind speed.

Figure 6 profiles are nearly linear in the Ln-Ln display and some of the measured have unexpected positive slopes. Tables 1 and 2 list MAPTIP and ASGASEX profiles, according to size, that had positive slopes. The fraction with positive slopes is given on the bottom row of each experiment's listing, i.e. 7/8 for MAPTIP's and 3/4 for

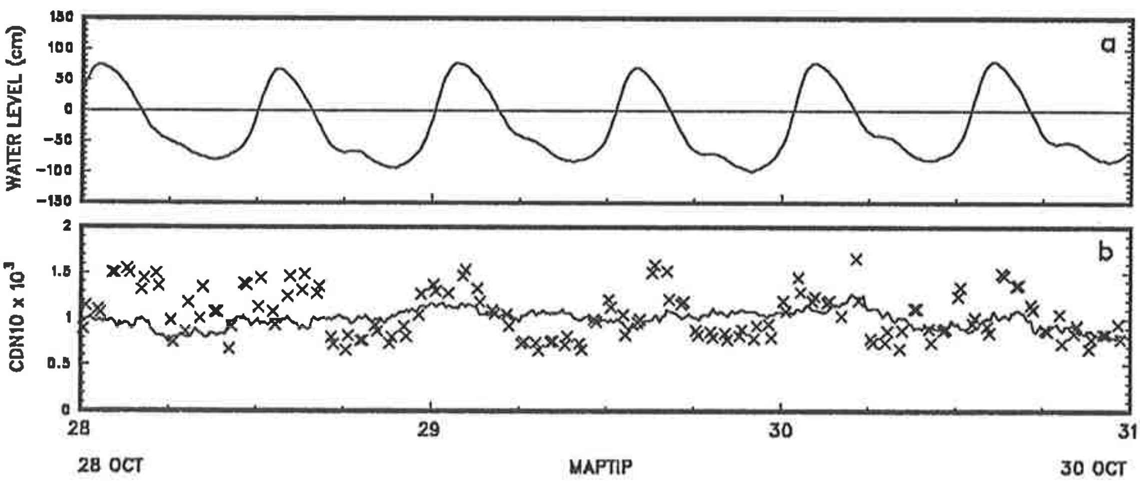

Figure 5.
Time series of a) water level measured at MPN and b) Buoy obtained neutral 10-meter drag coefficient, C_{D10N}.

Table 2 ASGASEX Profile Periods

date/time mo/day/UT	Wdir (°)	U m/s	RH %	Tair C	Tsea C	Radius (µm) 8	12	16	21	28	38	50	63	Tot	8-21 µm	28-62 µm
9/23/1445	355	4.3	84	15.8	16.7	x		x	x	x	x			5	3	2
9/24/0919	66	5.2	89	13.1	16.4									0	0	0
9/24/1540	18	9.1	81	15.1	16.5	x								1	1	0
9/15/1110	250	9.4	77	14.7	16.2	x								1	1	0
			Total Positive			3	0	1	1	1	1	0	0	7	5	2
			Total Profiles			4	3	4	4	4	2	0	0	21		
									Percent Positive						33%	

ASGASEX's 8 μm size bins. Equilibrium profiles for situations with a surface source, assumed in Eqn (1)/, should have negative slopes. Minimal slopes are expected for smaller aerosol sizes which have smaller V_d's and are more likely advected from a distance. Causes for positive slopes could be due to no surface production or advected aerosol, more likely at small sizes, or a non-equilibrium situation where upward transport exceeds downward transport plus gravitational settling, causing a maximum above the surface.

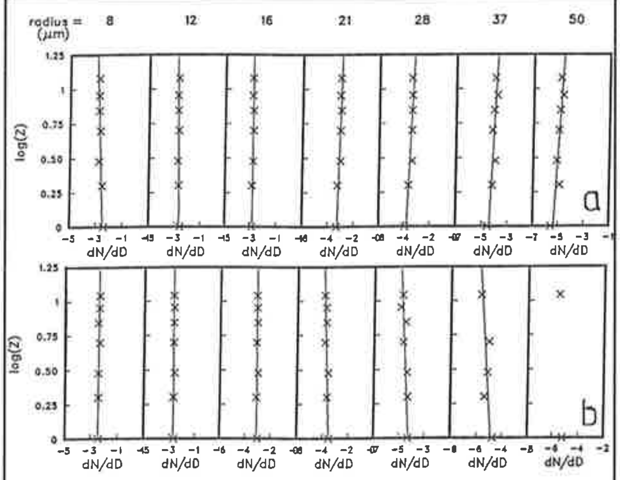

Figure 6.
Profiles and best fit regression lines of/for Ln(dN/dD) versus Ln(Z) for a) MAPTIP (10/20/13:28 UT) and b) ASGASEX (09/24/15:10). Profile nominal radii (m) is listed on top.

The MAPTIP (Table 1) fraction of positive slopes decreases as radii increases, as expected. However, MAPTIP's fraction with positive slopes is quite large, 46 out of 83 or 55% of the profiles. A possible reason for this MAPTIP result is that the influence of the surface production is diminished by advection from land; the airflow was always from the NE-E quadrant. Positive slope distributions in Table 1, MAPTIP periods sorted according to wind direction, seem to show an increase in positive slopes, particularly for larger sizes, when the wind direction is clockwise from 50 deg. The 13:46 UT 19 October, with a wind direction of 35 deg, is a definite exception to this rule since all 7 radii had positive slopes. However, that period also had the lowest wind speed, 2.1 m/s, so surface production was unlikely. Although the ASGASEX sample size is small, the ASGASEX fraction of positive profile slopes was significantly smaller, 33% versus 55%, Table 2. The most apparent aspect of ASGASEX positive slopes is that a light wind, 4.2 m/s, period was the only one that had them at radii greater than 8.5 μm.

4. RESULTS ON MODELING SURFACE-LAYER AEROSOL GRADIENTS

The Eqn (1) prediction for the profile gradients rather than concentrations at a given height is the feature being examined in the combined data set. Further, gradient is evaluated on the basis of the apparent deposition velocity, V_d, i.e.

$$V_d = \frac{[ku_*]\,[\mathrm{Ln}(X_2)-\mathrm{Ln}(X_1)]}{[\mathrm{Ln}(Z_2/Z_1) - \Psi(Z_2/L) + \Psi(Z_1/L)]} \quad (4)$$

where $\mathrm{Ln}(X_i)$'s were determined on the basis of regression-obtained coefficients and Z_i's values were 30 and 15 meters.

The appropriateness of Eqn (1) for describing near-surface aerosol profiles was evaluated on the basis of comparing V_d's calculated with Eqn (4) and available data with the gravitational settling rate, V_g,

i.e. $V_g = 2\,\rho\, g\, r^2 /(9\gamma)$ (5)

where γ is viscosity of air and ρ is density of aerosol

With Eqn (5), the aerosol is assumed to be in equilibrium with the local relative humidity. Further, we are neglecting the turbulent deposition rate which increases the V_d. The difference becomes less with increasing radius so that V_d is essentially determined by V_g for radii greater than 10 μm, [5]. In this analysis, 8.5 μm was the smallest size for which profiles were determined.

Comparisons of V_d's calculated with Eqn (4) with V_g's are shown in Figures 7a and 7b, for MAPTIP and ASGASEX respectively. The V_d's are based on both buoy inertial-dissipation determined u_*'s in Eqn (4) and on u_*'s determined with a bulk method [10] and MPN data. V_g dependence on the radii leads to vertical columns of data points, corresponding to the radii bins. There are 8 such columns for MAPTIP corresponding to radii from 8.5 to 62.5 μm and 6 for ASGASEX corresponding to radii from 8.5 to 37.5 μm. Pairs of V_d's from the two methods are also apparent since the dissipation datum point is slightly above (usually) the bulk data point in the column. Of course, an unpaired bulk data point means there was no buoy data. We include V_g's calculated with bulk u_*'s in this comparison because aerosol profiles were available for 6 periods listed in Table 1 before buoy data became available, from 10/19 through 10/25. Also, we want to examine the importance of the method for specifying u_*'s.

MAPTIP comparisons in Figure 7a show that V_d's are both greater and less than V_g. The spread around the identity line is within a factor of 3. There is a tendency for V_g to be less than V_d for larger radii, V_g>9 cm/s or r>20 μm. Additional examinations were done to explain the scatter. They showed that correcting V_g for turbulent deposition does not improve comparison agreement nor does restricting the comparison to MPN wind directions that are more northeasterly than easterly. With respect to the wind direction, the local wind direction may not be the best indicator of the trajectory. Trajectory analyses is being performed as a continuing step with this data.

ASGASEX comparisons in Figure 7b show V_d in agreement with V_g, with less scatter than for MAPTIP. The ASGASEX non-bulk u_* values were obtained from calculating the <u'w'> covariance from turbulent wind from MPN. This is normally referred to as the "direct" method. As for MAPTIP, V_d is generally less than V_g for V_g>9 cm/s or r>20 μm. We do not believe it is the different method, direct versus dissipation, that causes the apparent better agreement in the ASGASEX comparison because the bulk also has better agreement. ASGASEX definitely had the higher percentage of North Sea winds,

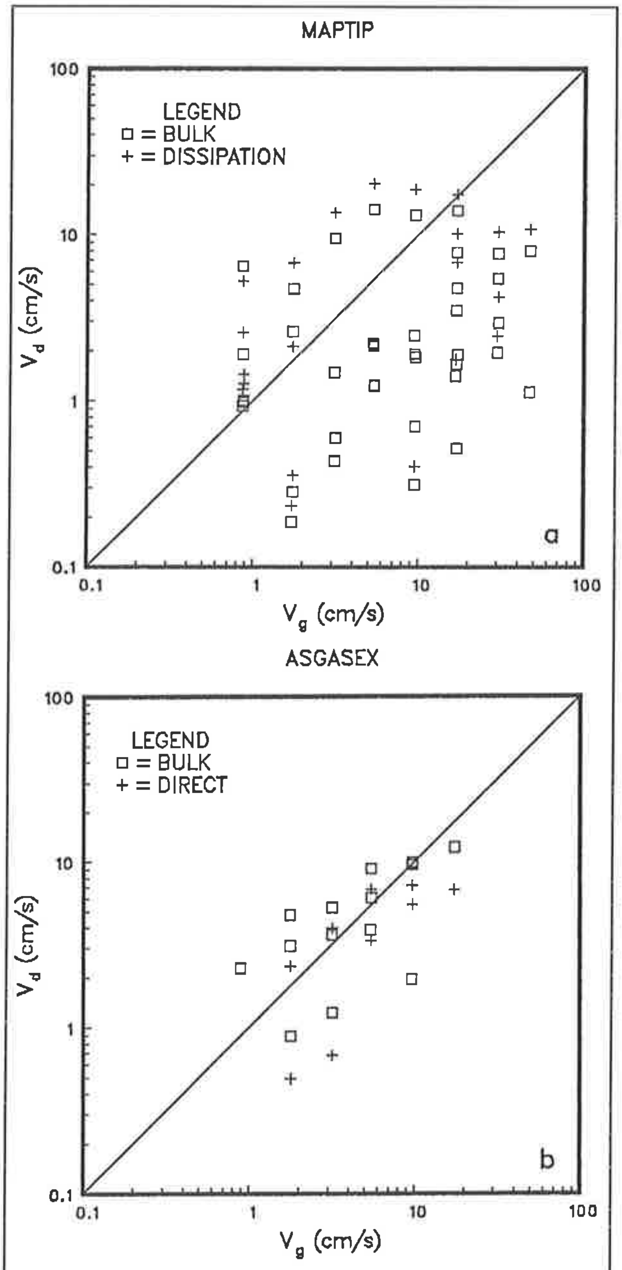

Figure 7.
Comparison of V_d and V_g for a) MAPTIP and b) ASGASEX. Dissipation/direct and bulk refer to method for estimating u* in Eqn (4).

only one was more clockwise than 50 deg, Table 2. Of course the one with the lowest wind speed, 1445 UT on 23 September, had 5 of the 7 positive slopes in ASGASEX. Because the sample size is small, trajectory analyses results have to be available before further interpretations can be made.

Although both MAPTIP and ASGASEX comparisons yielded reasonable agreement between the aerosol profile gradient calculated V_d's and the V_g's, we have to note the large fraction not included in Figure 7 due to positive slopes. Not included in Figure 7a (MAPTIP) were results from 46 of 83 profiles, or 55%, and in Figure 7b (ASGASEX) from 7 of 21 profiles, or 33%. We believe the positive slope profiles in MAPTIP were closely associated with the local wind direction, i.e. advection while the most apparent one in the small ASGASEX sample was definitely associated with low wind speed, i.e. no production. However, we can say that when the graduate is negative a simple model seems to exist.

These results are from a much more thorough examination on the representativeness and use of Eqn (1) than performed previously, by Davidson and Schutz [13]. The latter did not have the important aerosol profile data but inferred the correctness of Eqn (1) from single level data relying on varying L and u* instead of different Z values .

5. DISCUSSION

Combined surface layer turbulence and aerosol profile data sets were successfully obtained during a portion of the MAPTIP-IOP. Comparisons of the inertial-dissipation derived u* at the buoy with bulk values derived from the MPN data leads to the conclusion that MPN data are sufficient for characterizing MAPTIP-IOP periods when buoy data were not available. The characterization is required by a model for surface-layer aerosol profiles that is based on gravitational settling rate, V_g, turbulent transport, u*, and thermal stratification, Z/L.

An objective of this study has been to provide other MAPTIP-IOP participants an approach for estimating multi-radius profile gradients when MPN aerosol measurements were not made or not valid because of flow through the platform. In this regard, model prediction will always yield negative concentration gradients even though the actual gradients may be positive. The positive gradients will be more likely for smaller sizes, for light wind conditions, and for more easterly wind, clockwise from 45 deg.

Further studies will be useful with the combined data sets. These would lead to better understandings of the following influences,

a) air-mass trajectory,

b) relative humidity gradient, and

c) turbulent deposition.

6. ACKNOWLEDGEMENTS

Data collection and analyses in this work was funded under NRaD program element 62435N, RL3C Project RO35W82/01, Marine EO Effects, and by the MOD-NL (assignment A92KM615). Grants were obtained from NATO AC/243 (Panel 4) (Grants 6056 and 6092) and the US Office of Naval Research ONR (Grant N00014-91-J-1948) as contributions to the MAPTIP logistics costs. We thank staff persons at NPS and TNO-FEL who were involved in collection and analyses of the data; K. Jones, T. Neta, Leo Cohen, Lex van Eijk, F. Bastin. We also thank CDR L. van der Poel and his crew of the Tydeman who were instrumental in recovering and repairing the buoy. Rijkswaterstaat Directorate North Sea is gratefully acknowledged for making available MPN and the platform manager for their cooperation. This paper was written while KLD was a visiting Scientist at TNO-FEL.

7. REFERENCES

1. Gathman, S. G. and K. L. Davidson, "The Navy Oceanic Vertical Aerosol Model", NRaD TR-1634, December 1993, 107 pp.

2. Goroch, A. K., S. K. Burk, and K. L.. Davidson, "Stability Effects on Aerosol Size and Height Distributions", Tellus, 32, 1980, pp 245-250.

3. Fairall, C. W., and K. L. Davidson, "Dynamics and Modeling of Aerosols in the Marine Atmospheric Boundary Layer", in "Oceanic Whitecaps", D. Reidel Publishing Company, E. C. Monahan and G. Mac Niocaill (eds), 1986, pp 195-208.

4. Businger, J. A., J. C. Wyngaard, Y. Izumi, . E. F.. Bradely, "Flux-profile Relationships in the Atmospheric Surface Layer", J. of Atmos. Sci., 28, 1971, pp 181-189.

5. Fairall, C. W.. and S.E. Larsen, "Dry Deposition, Surface Production and Dynamics of Aerosols in the Marine Boundary Layer", Atmos. Envir., 18, pp 69-77, 1983.

6. Toba, Y., "On the Giant Sea-salt Particles in the Atmosphere, II. Theory of the Vertical Distribution in the 10 m over the Ocean", Tellus, 17, 1965, pp 365-382.

7. Skupniewicz, C. E. and K. L. Davidson, "Hot-film measurements from a small buoy: Surface stress estimates using the inertial-dissipation method", J. of Atmos. and Ocean. Tech., 8, 1991, pp 309-322.

8. Panofsky, H. A. and J. A. Dutton, "Atmospheric Turbulence", Wiley-Interscience, New York, N. Y., 1984, 397 pp.

9. Edson, J. B., C. W. Fairall, S. E. Larsen, and P. G. Metsasyer, "An Experimental and Theoretical Investigation of the Inertial-Dissipation Method for Computing Air-Sea Fluxes", J. of Geophys. Res., 96, 1991, pp 10689-10711.

10. Smith, S. D., R. Anderson, W. A.. Oost, C. Kraan, N. Maat, J. DeCosmo, K. B.. Katsaros, K. L. Davidson, K. Bumke, L. Hasse, and H. M. Chadwick , "Sea Surface Wind Stress and Drag Coefficients: The HEXOS Results", Boundary-Layer Meteorology, 60, 1992, pp 109-142.

11. De Leeuw, G., "Profiles of Aerosol Concentrations, Particle Size Distributions and Relative Humidity in the Atmospheric Surface Layer Over the Sea", Tellus, 42B, 1990, pp 342-354.

12. Oost, W. B., "The ASGASEX experiment", KNMI Technical Report, TR-161, 1994, 29 pp.

13. Davidson, K. L., and L. Schutz, "Observational Results on the Influence of Surface Layer and Inversion Entrainment on Surface Layer Marine Aerosol Number Density (1 μm)", Opt. Eng., 23, 1983, pp 45-49.

AGARD-CP-567

AGARD-CP-567

AGARD

ADVISORY GROUP FOR AEROSPACE RESEARCH & DEVELOPMENT

7 RUE ANCELLE, 92200 NEUILLY-SUR-SEINE, FRANCE

AGARD CONFERENCE PROCEEDINGS 567

Propagation Assessment in Coastal Environments

(l'Évaluation de la propagation en régions côtières)

Papers presented at the Sensor and Propagation Panel Symposium, held in Bremerhaven, Germany 19-22 September 1994.

NORTH ATLANTIC TREATY ORGANIZATION

Published February 1995

Distribution and Availability on Back Cover